ORIGINAL RESEARCH

Med J SDU / SDÜ Tıp Fak Derg ▸ 2026:33(2):136-144 ▸ doi: 10.17343/sdutfd.1793054

Electric Field-Induced Remodeling in Cardiac Tissue: Histopathological and BMP-2 Immunoreactivity Alterations Following High-Voltage Exposure in Rats

Zehra KÜÇÜKTEPE[1], Mustafa KARABACAK[2], Halil AŞÇI[3], Selçuk ÇÖMLEKÇİ[4], Özlem ÖZMEN[5]

[1] Suleyman Demirel University, Faculty of Medicine, Department of Cardiology, Isparta, Türkiye
[2] Suleyman Demirel University, Faculty of Medicine, Department of Cardiology, Isparta, Türkiye
[3] Suleyman Demirel University, Faculty of Medicine, Department of Pharmacology, Isparta, Türkiye
[4] Retired Electrical and Electronic Engineer, Isparta, Türkiye
[5] Burdur Mehmet Akif Ersoy University, Faculty of Veterinary, Department of Pathology, Burdur, Türkiye

Cite this article as: Küçüktepe Z, Karabacak M, Aşçı H, Çömlekçi S, Özmen Ö. Electric Field-Induced Remodeling in Cardiac Tissue: Histopathological and BMP-2 Immunoreactivity Alterations Following High-Voltage Exposure in Rats. Med J SDU 2026; 33(2): 136-144. Doi: 10.17343/sdutfd.1793054

Abstract

Objective

The 10 kV/m electric field, with a repetition frequency of 50 Hz and unidirectional pulsed (DC), which is accepted as the biological interaction limit by the World Health Organization, can also have an effect on cardiac tissues. 10 kV/m electric field exposure (pulsed wave shape) is increasingly seen both in the workplace and clinically. This study aimed to evaluate the structural and molecular responses of the heart to graded durations of 10 kV/m electric field (EF) exposure in rats.

Material and Method

Forty male Sprague-Dawley rats were randomly assigned to five groups (n = 8/group): control (0 min), and EF exposure for 1, 5, 15, or 30 minutes. Animals in the experimental groups were exposed to a pulsed electric field of 10 kV/m generated by a parallel-plate electrode system under standardized conditions.The pulses are unidirectional and have a repetition time of 20 ms (50 Hz). Hearts were harvested post-exposure and examined histopathologically. In addition, Bone Morphogenetic Protein-2 (BMP-2), vascular endothelial growth factor (VEGF), and fibroblast growth factor (FGF) immunohistochemical evaluation were performed, and immunopositivity was scored semi-quantitatively.

Results

Histopathological evaluation revealed intact myocardial architecture in control, 1-, 5-, and 15-minute groups. However, 30-minute EF exposure induced moderate hyperemia. Immunohistochemistry revealed minimal expression of BMP-2, VEGF, and FGF in early exposure groups, but BMP-2 showed focal upregulation in the 30 min group. VEGF and FGF remained unchanged.

Conclusion

Prolonged monophasic, high-intensity pulsed electric field exposure induces early signs of microvascular remodeling in cardiac tissue, reflected histologically by hyperemia and molecularly by increased BMP-2 expression. These findings suggest BMP-2 may serve as an ear-ly biomarker of cardiac remodeling in electrically active environments or device interfaces, such as pacemaker implantation zones.

Keywords: BMP-2, Cardiac remodeling, Electric field, Immunohistochemistry, Rat

Correspondence: Z.K. / zehrakucuktepe@sdu.edu.tr
Received: 09.10.2025 • Accepted: 09.04.2026
ORCID IDs of the Authors: Z.K: 0009-0005-4485-5574; M.K: 0000-0001-6879-5522; H.A: 0000-0002-1545-035X; S.Ç: 0000-0003-1389-6435; Ö.Ö: 0000-0002-1835-1082

Introduction

The mammalian heart exhibits a remarkable capacity for structural and functional adaptation to diverse physical stimuli, including pressure, stretch, and, more recently, externally applied electric fields (EFs) (1). While EFs are traditionally associated with electrophysiological control via pacemakers and defibrillators, emerging research highlights their potential to modulate cellular signaling, vascular tone, and extracellular matrix remodeling (2-4). However, the biological responses of myocardial tissue to sustained high-intensity EF exposure remain incompletely understood. High-intensity electric fields can alter cell membrane potentials, activate ion channels, and stimulate intracellular pathways, leading to calcium influx, MAPK activation, and transcription of stress-related genes, such as those encoding bone morphogenetic proteins (5-8). Among these, Bone Morphogenetic Protein-2 (BMP-2) has garnered attention for its roles in both bone and cardiac tissues. In the heart, BMP-2 is involved in embryonic development, fibroblast activation, and post-infarct remodeling (9-13). BMP-2 expression is typically low under physiological conditions but increases in response to myocardial injury or stretch, suggesting it may act as a sensor of biomechanical stress. These structural adaptations are thought to stem not only from mechanical irritation but also from chronic micro-electric field exposure, yet the molecular mechanisms remain elusive. Understanding whether such electrical environments provoke early, non-lethal changes in myocardial biology, including upregulation of pro-remodeling factors like BMP-2, is essential for optimizing the safety and efficacy of cardiac electroceuticals (14-16).

Experimental and clinical studies have demonstrated that pacemaker or implantable cardioverter-defibrillator (ICD) leads may induce localized fibrotic remodeling and even alter conduction patterns around the electrode site (17-19). Previous EF-exposure studies in non-cardiac tissues have demonstrated voltage- and time-dependent expression of VEGF, TNF-α, and SPARC (osteonectin), markers of angiogenesis, inflammation, and matrix turnover (20-22). Whether similar processes are activated in the heart, a tissue highly sensitive to ionic flux and metabolic stress, is unknown (23). Given this context, the present study aimed to evaluate the histopathological and immunohistochemical effects of graded-duration high-density (10 kV/m) electric field exposure on rat myocardial tissue. Specifically, we assessed changes in vascular integrity and BMP-2, FGF, and VEGF expression as indicators of early remodeling. Our findings may help elucidate the interface between electrical stimuli and cardiac structural biology, with implications for pacemaker-tissue interactions and bioelectronic medicine.

Material and Method

Animals and Experimental Design

Forty adult male Sprague-Dawley rats (10–12 weeks old; 250–300 g) were obtained from the Isparta Süleyman Demirel University Experimental Animal Center. All experiments complied with the Animal Research: Reporting of In Vivo Experiments (ARRIVE) 2.0 guidelines. Animals were housed under standard laboratory conditions (22 ± 2°C, 12-hour light/dark cycle, ad libitum feeding). Following acclimatization, rats were randomly divided into five groups (n = 8 per group) based on EF exposure duration:

Group I – Control (0 min, no EF exposure): Rats in this group were handled identically to the other groups, including placement in the exposure chamber, but no electrical voltage was applied. This group served as the baseline reference to assess the natural morphology and biomarker expression of cardiac tissue without any electrical influence.

Group II – 1-minute exposure: Animals in this group were exposed to a high-density direct current electric field of 10 kV/m for exactly 1 minute. This short-duration exposure aimed to model acute, subthreshold electrical stimulation, such as may occur during brief diagnostic pacing procedures or accidental low-level environmental exposure.

Group III – 5-minute exposure: This group received a moderate-duration EF exposure of 5 minutes. It was designed to investigate whether a slight extension in exposure duration leads to incremental histopathological or molecular changes, potentially mimicking therapeutic stimulation parameters used in emerging electroceutical technologies.

Group IV – 15-minute exposure: Rats in this group underwent 15 minutes of continuous EF exposure, representing a prolonged but clinically plausible exposure duration in cases such as malfunctioning pacing devices or therapeutic protocols involving field modulation. This group served as a critical mid-point to detect threshold effects in tissue remodeling.

Group V – 30-minute exposure: This final group was exposed to 10 kV/m for 30 minutes, modeling subacute high-density electric field exposure conditions. This duration was selected based on preliminary studies indicating the likelihood of early tissue-level changes, including microvascular alterations and

pro-remodeling marker expression, without overt cell death.

Electric Field Application Protocol

A 10 kV/m intensity electric field, which has the pulses unidirectional and have a repetition time of 20 ms (50 Hz, monophasic DC), was generated using a custom-built parallel plate system. High voltage (5.5 kVdc) is required, and this was supplied by the control box. This control box has been custom-built. The animal cages are sized 26x43x15 cm. Due to all the parallel cages being spaced 50 cm apart, we can get the EF intensity as a value of 10 kV/m. EF exposure was conducted using a custom-designed high-voltage parallel plate system engineered to generate a uniform field. No direct contact occurred between electrodes and rats. Animals were euthanized 1 hour after exposure for tissue analysis.

The selected electric field intensity was chosen based on previous experimental studies reporting biological interaction thresholds without inducing thermal or necrotic injury. Exposure durations were designed to capture acute-to-subacute responses and to identify potential temporal thresholds for early myocardial remodeling.

Histopathological Method

Euthanasia was performed by decapitation under deep anesthesia induced with an intraperitoneal combination of 10 mg/kg Xylazine (Xylazinbio 2%, Bioveta, Czech Republic) and 90 mg/kg Ketamine (Ketalar, Pfizer, Türkiye), in accordance with institutional and international ethical guidelines. The depth of anesthesia was confirmed by the absence of pedal and corneal reflexes before proceeding with euthanasia by decapitation. Heart samples were collected during necropsy and preserved in a 10% neutral formalin solution. The heart samples were then embedded in paraffin wax following standard tissue processing using an automated tissue processing device (Leica ASP300S, Wetzlar, Germany). Subsequently, 5 µm thick sections were cut from the paraffin blocks using a fully automated rotary microtome (Leica RM2155, Leica Microsystems, Wetzlar, Germany). These sections were stained with hematoxylin and eosin (H&E), cover-slipped, and examined under light microscopy. Histological lesions in the hearts were graded semi-quantitatively using an ordinal grading system. This evaluation included assessment of hyperemia, hemorrhage, inflammatory cell infiltrations, and degenerative necrotic changes in myocardial cells. Lesions were classified as normal (score = 0), mild (1), moderate (2), or severe (3) according to the semi-quantitative grading system (Table 1).

Immunohistochemical Examination

For immunohistochemical analysis, three series of slices were cut from the paraffin blocks and mounted on slides coated with poly-L-lysine. Sections were then subjected to immunohistochemical staining following the manufacturer's instructions to assess the expression of BMP-2, FGF, and VEGF using the streptavidin-biotin-peroxidase method (HRP/DAB). Primary antibodies used were BMP-2 (BMP2 Antibody - #AF5163, Affinity Bioscience, Canada), FGF (FGF-2 Antibody (C-2): sc-74412, Santa Cruz, Texas, USA), and VEGF (VEGFA antibody, #AF5131; Affini-

Table 1 Histopathological and immunohistochemical scores and affections

		Scores			
		0	**1**	**2**	**3**
Evaluations	**Histopathological**	normal myocardial architecture; no evidence of degeneration, necrosis, or inflammatory infiltration	mild myocardial alterations, including slight myofibrillar disorganization and minimal interstitial edema	moderate myocardial damage characterized by myocyte degeneration, inflammatory cell infiltration, and interstitial edema	severe myocardial injury with widespread myocyte necrosis, marked inflammatory infiltration, hemorrhage,
	Immunohistochemical	no expression	focal and weak staining	diffuse and weak staining	diffuse and marked staining

ty Bioscience, Canada) at a 1/100 dilution. Immunohistochemistry was performed using a streptavidin–alkaline phosphatase conjugate and a biotinylated secondary antibody following a 60-minute incubation with the primary antibodies. Mouse and Rabbit Specific HRP/DAB IHC Detection Kit - Micro-polymer (ab236466) from Abcam (Cambridge, UK) was used as the secondary antibody, and diaminobenzidine (DAB) was employed as the chromogen. For negative controls, antigen dilution solution was applied instead of primary antibodies. Each evaluation was conducted on blinded samples by a specialized pathologist from another university.

At an objective magnification of x40, the IHC expressions were scored on a scale of 0-3. Accordingly, 0 indicates no expression, 1 indicates focal and weak staining, 2 indicates diffuse and weak staining, and 3 indicates diffuse and marked staining (Table 1). The ImageJ 1.48 software (National Institutes of Health, Bethesda, MD) was used to determine the positive immunohistochemical reaction. Olympus CX41 microscope was used for photographing the results, and the Database Manual Cell Sens Life Science Imaging Software System (Olympus Corporation, Tokyo, Japan) was used for microphotography.

For histopathological and immunohistochemical analyses, three non-consecutive sections were obtained from each paraffin-embedded cardiac tissue block per animal. From each section, at least five randomly selected, non-overlapping high-power fields (HPFs; ×400 magnification) were evaluated, resulting in a minimum of 15 fields analyzed per animal. All histopathological and IHC evaluations were performed twice by a single experienced pathologist who was blinded to the experimental groups. To ensure consistency, the assessments were repeated at different time points, and the final scores were determined based on concordant findings. Representative photomicrographs were selected to accurately reflect the median histopathological and immunohistochemical scores of each experimental group, while avoiding areas affected by sectioning artifacts, edge effects, or staining irregularities. Image acquisition parameters were standardized across all groups to maintain consistency and comparability.

For each animal, at least three non-consecutive sections were analyzed, and five randomly selected high-power fields per section were evaluated.

Statistical Analysis

The results were analyzed with the Kruskal-Wallis test followed by the Dunn's post hoc test. Statistical analysis was performed using GraphPad Prism version 10.1 software (San Diego, California, USA). Differences were considered significant for $p < 0.05$. All results are expressed as median ± interquartile range. Although histopathological and immunohistochemical scores were ordinal in nature, data distribution was assessed using the Shapiro–Wilk test and showed no significant deviation from normality. Therefore, parametric analysis (one-way ANOVA followed by Tukey's post hoc test) was applied. To ensure robustness, non-parametric Kruskal–Wallis analysis was also performed as a sensitivity analysis, yielding consistent results.

Results

Histopathology Findings

Light microscopic evaluation of hematoxylin and eosin (H&E)-stained myocardial sections revealed a clear time-dependent response to electric field exposure. In the control group (0 min), myocardial tissue exhibited normal histoarchitecture: cardiomyocytes were elongated, eosinophilic, and radially arranged with well-preserved intercalated discs. The endomysial and perimysial connective tissue compartments were intact, and the capillary network was dense yet not dilated.

Similarly, the 1-minute and 5-minute exposure groups showed no remarkable histological deviations compared to controls. Cardiomyocyte alignment and nuclear morphology were preserved, with no evidence of edema, hemorrhage, or inflammatory infiltration detected.

In the 15-minute exposure group, cardiac tissue largely retained its overall architecture; however, some specimens exhibited early vascular changes, including mild capillary dilation and increased erythrocyte density in the interstitial spaces.

The most notable alterations were observed in the 30-minute exposure group, where myocardial sections showed moderate hyperemia with expanded vascular lumens and increased erythrocyte extravasation into the interstitial matrix. Cardiomyocytes in these regions demonstrated slightly widened intercellular spaces, suggestive of early tissue stress or perfusion imbalance. Notably, no necrosis, fibrosis, or inflammatory cell infiltration was detected in any group, indicating a non-lethal, adaptive tissue response rather than overt injury (Fig 1 and 2).

Immunohistochemical Examination

Immunohistochemical staining was conducted to as-

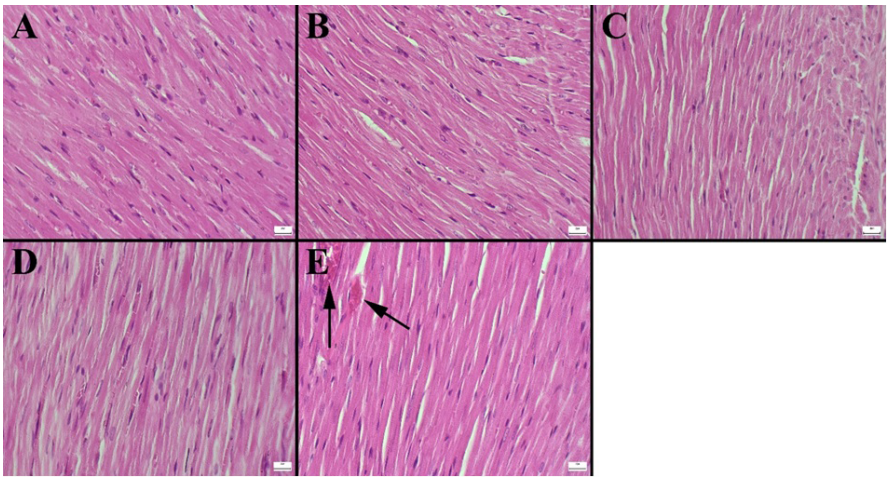

Figure 1

Representative histopathological figures of hearts between the groups. Normal myocardial tissue histology in (A) control, (B) 1 min, (C) 5 min, (D) 15 min group, (E) Moderate hyperemia (arrows) in the 30 min group, HE, scale bars = 20 µm.

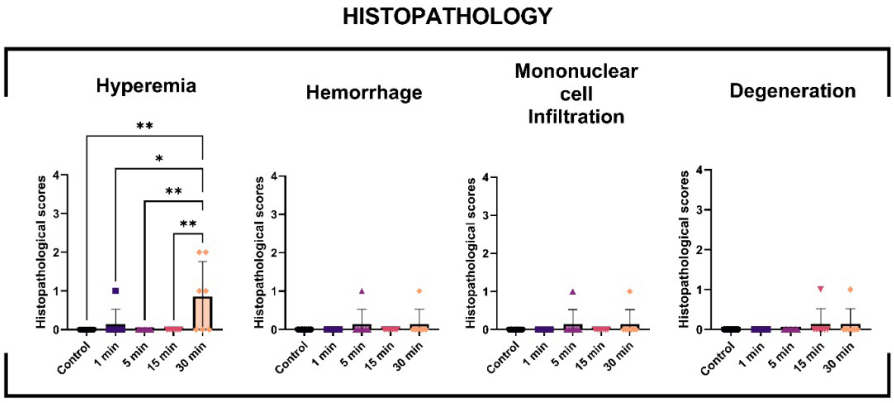

Figure 2

Statistical graphs illustrating the histopathological scores of hyperemia, hemorrhage, inflammatory infiltration, and degeneration across the experimental groups. Data are presented as median ± interquartile range (n = 8). Asterisks (*) and (**) denote statistically significant differences compared with the control group at $p < 0.05$ and $p < 0.001$, respectively.

sess expression of BMP-2, VEGF, and FGF as markers of remodeling, angiogenesis, and growth factor activation in myocardial tissue following EF exposure.

BMP-2 Expression

In the control, 1-minute, 5-minute, and 15-minute groups, BMP-2 immunoreactivity was either absent or limited to weak, focal cytoplasmic staining (score = 0–1). However, in the 30-minute group, moderate, diffuse BMP-2 expression (score = 2–3) was observed in cardiomyocytes and perivascular regions. Cytoplasmic positive expression was particularly prominent in regions with pre-existing hyperemia, suggesting a spatial correlation between vascular response and BMP-2 activation. This change was statistically significant compared to all other groups ($p < 0.01$) (Fig 3).

VEGF and FGF Expression

Both VEGF and FGF-2 markers showed no statistically significant differences among exposure groups. While occasional weak VEGF immunoreactivity was noted in perivascular endothelial cells in the 30-minute group, these findings did not reach statistical significance ($p > 0.05$). FGF expression remained low and diffuse in all groups, suggesting that electric field exposure at these parameters did not induce angiogenic or fibroblastic transformation within the observed period (Fig 4).

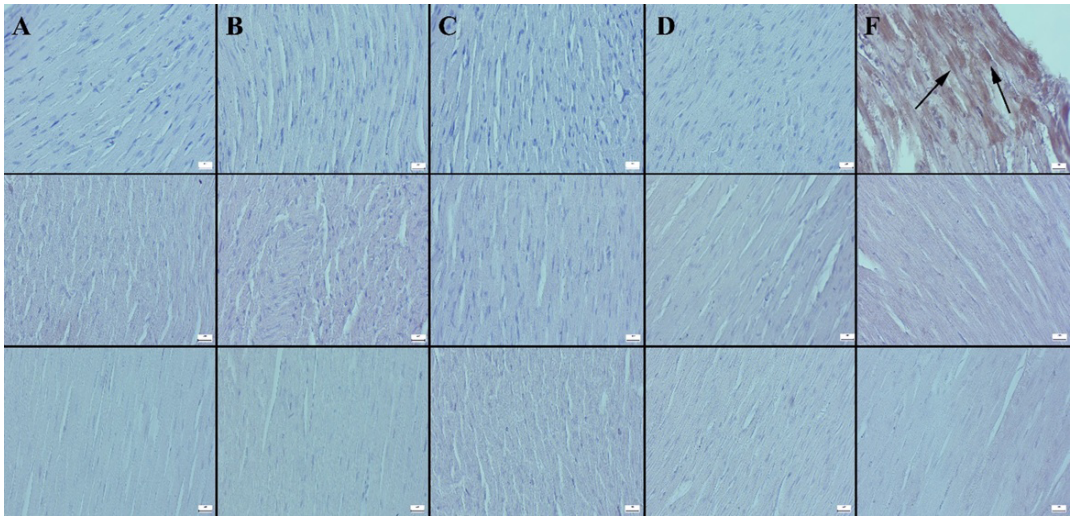

Figure 3

Immunohistochemical BMP-2 (upper row), FGF (medium row) and VEGF (below row) expressions of hearts between the groups. Negative expression (A) in Con group, (B) 1 min group, (C) 5 min, (D) 15 min and (E) slight to moderate increase in BMP-2 in 30 min group (arrow) Streptavidin biotin peroxidase method, scale bars=20µm.

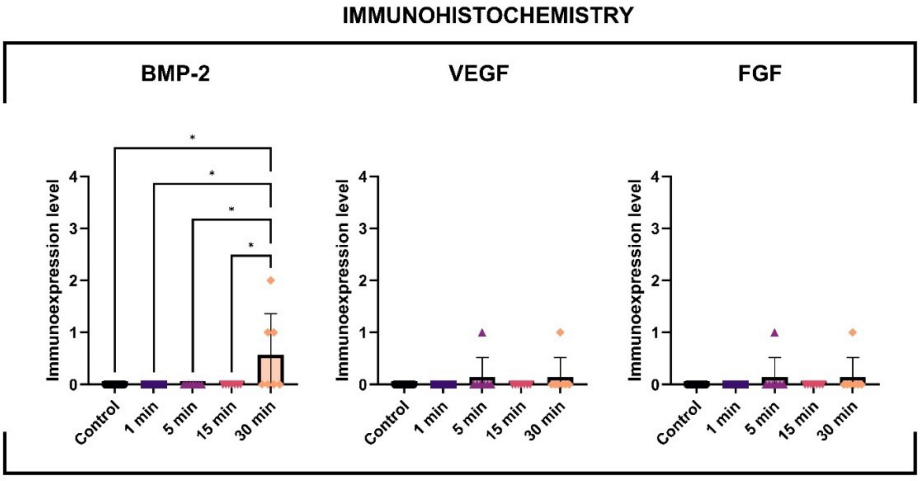

Figure 4

Statistical analysis graphs showing the immunohistochemical expression levels of BMP-2, VEGF, and FGF in cardiac tissue. A statistically significant increase in BMP-2 expression was observed exclusively in the 30-minute electric field (EF) exposure group ($p < 0.05$), suggesting time-dependent molecular remodeling. In contrast, no significant differences were detected in VEGF or FGF expression among groups. Data are presented as median ± interquantile range (n = 8). Asterisks (*) denote statistically significant differences compared to the control group.

Discussion

This study provides novel insights into the effects of graded-duration high-voltage electric field (EF) exposure on myocardial structure and molecular remodeling in rats. Using both histopathological and immunohistochemical approaches, we demonstrate that Extremely Low Frequency (50 Hz), pulsed 10 kV/m EF, when applied for 30 minutes, induces moderate hyperemia and significant upregulation of BMP-2 expression in cardiac tissue, without overt necrosis or inflammation. These findings suggest that electric

fields, even in the absence of thermal or direct contact injury, may provoke adaptive changes in the myocardium via molecular signaling pathways.

Histologically, myocardial tissue exhibited a time-dependent response to EF exposure. While shorter exposures (1–15 min) did not elicit structural abnormalities, 30-minute exposure led to focal vascular dilation and hyperemia, hallmarks of early vascular reactivity. This vascular change, in the absence of inflammatory infiltration or cardiomyocyte degeneration, suggests a subclinical physiological response rather than overt injury. Similar vascular responses to sub-threshold stimuli have been reported in skeletal muscle and endothelium under electrical stimulation (24). Among the most notable findings was the increased expression of BMP-2 in myocardial cells after 30-minute exposure. BMP-2, a member of the TGF-β superfamily, has well-established roles in cardiac development, post-injury remodeling, and fibroblast activation (25). In our study, the spatial distribution of BMP-2—localized to areas of vascular congestion—supports the hypothesis that EF exposure can activate mechano-sensitive or voltage-gated pathways involved in tissue remodeling. Mechanistically, EF exposure may modulate intracellular ion homeostasis, particularly calcium influx, which is a known trigger for MAPK and Smad signaling cascades that regulate BMP transcription (26).

Voltage-gated calcium channels in cardiomyocytes are responsive to external field gradients, and their sustained activation has been implicated in adaptive gene expression changes during biomechanical stress (27, 28). Interestingly, neither VEGF nor FGF showed significant changes among exposure groups. VEGF is typically upregulated in hypoxia-driven angiogenesis, and FGF is associated with fibrogenic or proliferative signaling (29, 30). The absence of change in these markers reinforces the notion that EF exposure in this model triggered a selective, early-stage remodeling program dominated by BMP-2, rather than a generalized injury or ischemic response. Importantly, the present model does not aim to replicate the chronic, localized electrode–tissue interface seen in implanted cardiac devices, but rather to provide a controlled platform for identifying early, whole-tissue molecular responses to electric field exposure. These findings hold particular relevance in the context of cardiac implantable electronic devices (CIEDs). Chronic low-level electrical stimulation from pacemaker or ICD leads has been associated with local myocardial fibrosis and altered signal conduction at the lead-tissue interface (31). Our findings suggest that such effects may be preceded by molecular remodeling, including BMP-2 induction, even in the absence of clinical symptoms or histological damage. This model may also serve as a foundational platform for studying electroceutical interventions. With growing interest in bioelectronic medicine, understanding how the myocardium responds to different EF parameters is essential for optimizing device safety and efficacy (32, 33). Our results suggest that exposure duration is a critical determinant of the myocardial response, with 30 minutes representing a possible threshold for molecular activation.

From a translational perspective, BMP-2 upregulation could serve as a potential biomarker of subclinical myocardial remodeling. Early detection of BMP-2 expression in patients undergoing chronic EF exposure whether therapeutic or environmental might offer predictive insights into subsequent tissue adaptation or dysfunction (34-36). Moreover, the absence of inflammatory or necrotic changes in our study distinguishes EF-induced remodeling from classical injury models, such as ischemia-reperfusion or myocarditis. This positions EF exposure as a unique mechanobiological stimulus that preferentially engages adaptive, rather than destructive, tissue responses.

The lack of histological changes in 1, 5, and 15-minute groups underscores the importance of exposure duration in determining biological outcomes. These results align with prior work in reproductive tissues and nerve models, where duration-dependent effects of EF on cytokine and growth factor expression were similarly observed (37-39).

Another notable aspect is the consistency of findings across both morphological and molecular analyses. BMP-2 upregulation coincided with regions of mild hyperemia, reinforcing the correlation between structural and molecular adaptations. This coherence strengthens the validity of BMP-2 as a reliable readout of EF-induced myocardial stress. Our findings also provoke questions regarding the reversibility of EF-induced BMP-2 expression. Is this activation transient and reversible, or could it lead to persistent structural remodeling? Longitudinal studies with extended post-exposure intervals would be invaluable in addressing this. The implications of these findings may extend beyond pacemaker technology. In electrophysiological procedures such as cardiac ablation, even brief field exposure can provoke localized remodeling. Identifying markers such as BMP-2 could help delineate therapeutic versus adverse effects in such contexts.

Limitations of this study include the absence of biochemical assays (e.g., ELISA or qRT-PCR) to confirm

protein expression levels and lack of functional cardiac assessments (e.g., ECG or echocardiography). However, the alignment of histopathological and immunohistochemical data offers a robust preliminary foundation.

In summary, our results demonstrate that prolonged high-voltage electric field exposure elicits selective molecular remodeling in the heart, primarily via BMP-2 upregulation and microvascular adaptation. These changes occur in the absence of overt structural damage, suggesting a physiological but potentially progressive tissue response. Further studies are warranted to explore the long-term implications and therapeutic modulation of such remodeling in clinical contexts.

Conclusion

This study demonstrates that exposure to a 10 kV/m, ELF pulsed electric field for 30 minutes results in moderate microvascular changes and a significant upregulation of BMP-2 expression in rat myocardial tissue, in the absence of overt necrosis or inflammation. These findings highlight the sensitivity of cardiac tissue to prolonged electric field exposure and suggest a potential mechanobiological mechanism of subclinical remodeling. The selective induction of BMP-2-without concurrent changes in VEGF or FGF-implies that specific intracellular signaling pathways, possibly calcium or voltage-gated mechanisms, may mediate this effect. Given the growing clinical use of cardiac implantable electronic devices and emerging bioelectronic medicine strategies, understanding the safe thresholds and biological impacts of electric fields on the heart is of increasing importance. Future studies are needed to determine the long-term consequences of such remodeling and whether BMP-2 could serve as a biomarker or therapeutic target in electroceutical cardiology.

Conflict of Interest Statement
The authors have no conflicts of interest to declare.

Ethical Approval
All experiments were performed under the guidelines for animal research from the National Institutes of Health and were approved by the Committee on Animal Research of Isparta Süleyman Demirel University (Ethic No:18.09.2025/623).

Funding
This study was supported by Isparta Süleyman Demirel University Scientific Research Projects Coordination Unit (project code TSG-2024-9515).

Availability of Data and Materials
The datasets generated and/or analyzed during the current study are available from the corresponding author upon reasonable request

Artificial Intelligence Statement
The authors declare that they have not used any type of generative artificial intelligence for the writing of this manuscript, nor for the creation of images, graphics, tables, or their corresponding captions.

Authors Contributions
ZK: Conceptualization; Data curation; Formal analysis; Investigation; Methodology; Writing-original draft.

MK: Validation; Visualization.

HA: Investigation; Validation; Writing-original draft.

SÇ: Data curation; Formal analysis; Writing- review & editing.

ÖÖ: Data curation; Visualization; Formal analysis.

References

1. Quinn TA, Kohl P. Cardiac Mechano-Electric Coupling: Acute Effects of Mechanical Stimulation on Heart Rate and Rhythm. Physiol Rev. 2021 Jan 1;101(1):37-92. doi: 10.1152/physrev.00036.2019. Epub 2020 May 7. PMID: 32380895.
2. Ye Z, Li Y, Zhao Y, et al. Correction to "Effect of Exogenous Electric Stimulation on the Cardiac Tissue Function in Situ Monitored by Scanning Electrochemical Microscopy". Anal Chem 2023 Jun 6;95(22):8744-8745. doi: 10.1021/acs.analchem.3c02009. Epub 2023 May 23. Erratum for: Anal Chem. 2023 Mar 14;95(10):4634-4643. doi: 10.1021/acs.analchem.2c04758. PMID: 37220385.
3. Katoh K. Effects of Electrical Stimulation of the Cell: Wound Healing, Cell Proliferation, Apoptosis, and Signal Transduction. Med Sci (Basel) 2023;11(1):11. doi: 10.3390/medsci11010011. PMID: 36810478; PMCID: PMC9944882.
4. Bielfeldt M, Rebl H, Peters K, et al. Sensing of physical factors by cells: electric field, mechanical forces, physical plasma and light—importance for tissue regeneration. Biomedical Materials & Devices. 2023;1(1):146-61.
5. Kaynak A, N'Guessan KF, Patel PH, et al. Electric Fields Regulate In Vitro Surface Phosphatidylserine Exposure of Cancer Cells via a Calcium-Dependent Pathway. Biomedicines. 2023;11(2):466. doi: 10.3390/biomedicines11020466. PMID: 36831002; PMCID: PMC9953458.
6. Aguilar AA, Ho MC, Chang E, et al. Permeabilizing Cell Membranes with Electric Fields. Cancers (Basel) 2021 May 10;13(9):2283. doi: 10.3390/cancers13092283. PMID: 34068775; PMCID: PMC8126200.
7. Hanna H, Andre FM, Mir LM. Electrical control of calcium oscillations in mesenchymal stem cells using microsecond pulsed electric fields. Stem Cell Res Ther 2017 Apr 20;8(1):91. doi: 10.1186/s13287-017-0536-z. PMID: 28424094; PMCID: PMC5397732.
8. Heng BC, Bai Y, Li X, et al. The bioelectrical properties of bone tissue. Animal Model Exp Med. 2023 Apr;6(2):120-130. doi: 10.1002/ame2.12300. Epub 2023 Mar 1. PMID: 36856186; PMCID: PMC10158952.

9. Ma L, Lu MF, Schwartz RJ, et al. Bmp2 is essential for cardiac cushion epithelial-mesenchymal transition and myocardial patterning. Development. 2005 Dec;132(24):5601-11. doi: 10.1242/dev.02156. PMID: 16314491.
10. Rivera-Feliciano J, Tabin CJ. Bmp2 instructs cardiac progenitors to form the heart-valve-inducing field. Dev Biol. 2006 Jul 15;295(2):580-8. doi: 10.1016/j.ydbio.2006.03.043. Epub 2006 Apr 4. PMID: 16730346; PMCID: PMC2680002.
11. Docshin PM, Karpov AA, Mametov MVet al. Mechanisms of Regenerative Potential Activation in Cardiac Mesenchymal Cells. Biomedicines 2022 May 31;10(6):1283. doi: 10.3390/biomedicines10061283. PMID: 35740305; PMCID: PMC9220771.
12. Hanna A, Frangogiannis NG. The Role of the TGF-β Superfamily in Myocardial Infarction. Front Cardiovasc Med. 2019 Sep 18;6:140. doi: 10.3389/fcvm.2019.00140. PMID: 31620450; PMCID: PMC6760019.
13. Docshin P, Panshin D, Malashicheva A. Molecular Interplay in Cardiac Fibrosis: Exploring the Functions of RUNX2, BMP2, and Notch. Rev Cardiovasc Med. 2024 Oct 16;25(10):368. doi: 10.31083/j.rcm2510368. PMID: 39484128; PMCID: PMC11522771.
14. Csiszar A, Lehoux S, Ungvari Z. Hemodynamic forces, vascular oxidative stress, and regulation of BMP-2/4 expression. Antioxid Redox Signal. 2009 Jul;11(7):1683-97. doi: 10.1089/ars.2008.2401. PMID: 19320562; PMCID: PMC2842584.
15. Tokola H, Rysä J, Pikkarainen S, Hautala N, et al. Bone morphogenetic protein-2--a potential autocrine/paracrine factor in mediating the stretch activated B-type and atrial natriuretic peptide expression in cardiac myocytes. Mol Cell Endocrinol 2015 Jan 5;399:9-21. doi: 10.1016/j.mce.2014.09.003. Epub 2014 Sep 10. PMID: 25218476.
16. Howden R. McCann Hartzell K. Gladwell W., et al. Heart Rate and QT Interval Responses to Hyperoxia in Bmp 2 and Bmp 4 Heterozygous Mice (Poster Presentation). American Thoracic Society, Cellular And Molecular Aspects of Acute Lung Injury. 2009; A3567. Am J Respir Crit Care Med, 2009;179:A3567
17. Hopman LHGA, Beunder KP, Borodzicz-Jazdzyk S, et al. Loss of capture of conduction system pacemaker caused by fibrosis surrounding the lead: a case report. BMC Cardiovasc Disord. 2023 Dec 19;23(1):621. doi: 10.1186/s12872-023-03656-3. PMID: 38114911; PMCID: PMC10729341.
18. Keiler J, Schulze M, Sombetzki M, et al. Neointimal fibrotic lead encapsulation. Clinical challenges and demands for implantable cardiac electronic devices. J Cardiol. 2017 Jul;70(1):7-17. doi: 10.1016/j.jjcc.2017.01.011. PMID: 28583688.
19. Crea P, Cocuzza F, Bonanno S, et al. New Diseases Related to Cardiac Implantable Electronic Devices (CIEDs): An Overview. J Clin Med. 2025 Feb 17;14(4):1322. doi: 10.3390/jcm14041322. PMID: 40004852; PMCID: PMC11856071.
20. Chen Y, Ye L, Guan L, et al. Physiological electric field works via the VEGF receptor to stimulate neovessel formation of vascular endothelial cells in a 3D environment. Biol Open. 2018 Sep 19;7(9):bio 035204. doi: 10.1242/bio.035204. PMID: 30232195; PMCID: PMC6176943.
21. Mahaki H, Jabarivasal N, Sardanian K, et al. Effects of Various Densities of 50 Hz Electromagnetic Field on Serum IL-9, IL-10, and TNF-α Levels. Int J Occup Environ Med. 2020 Jan 1;11(1):24-32. doi: 10.15171/ijoem.2020.1572. Epub 2019 Oct 20. PMID: 31647056; PMCID: PMC7024597.
22. López-Morales GI, Zajac JM, Flick J, et al. Quantum embedding study of strain-and electric-field-induced Stark effects on the NV− center in diamond. Physical Review B. 2024;110(24):245127.
23. Kos B, Mattison L, Ramirez D, et al. Determination of lethal electric field threshold for pulsed field ablation in ex vivo perfused porcine and human hearts. Front Cardiovasc Med. 2023 Jun 23;10:1160231. doi: 10.3389/fcvm.2023.1160231. PMID: 37424913; PMCID: PMC10326317.
24. Zhao M, Bai H, Wang E, et al. Electrical stimulation directly induces pre-angiogenic responses in vascular endothelial cells by signaling through VEGF receptors. J Cell Sci. 2004 Jan 26;117(Pt 3):397-405. doi: 10.1242/jcs.00868. Epub 2003 Dec 16. PMID: 14679307; PMCID: PMC1459284.
25. Docshin P, Bairqdar A, Malashicheva A. Interplay between BMP2 and Notch signaling in endothelial-mesenchymal transition: implications for cardiac fibrosis. Stem Cell Investig. 2023 Sep 28;10:18. doi: 10.21037/sci-2023-019. PMID: 37842185; PMCID: PMC10570623.
26. Humeres C, Venugopal H, Frangogiannis NG. Smad-dependent pathways in the infarcted and failing heart. Curr Opin Pharmacol 2022 Jun;64:102207. doi: 10.1016/j.coph.2022.102207. PMID: 35367786; PMCID: PMC9167749.
27. Tomida S, Ishima T, Nagai R, et al. T-Type Voltage-Gated Calcium Channels: Potential Regulators of Smooth Muscle Contractility. Int J Mol Sci 2024 Nov 19;25(22):12420. doi: 10.3390/ijms252212420. PMID: 39596484; PMCID: PMC11594734.
28. Salvage SC, Habib ZF, Matthews HR, et al. Ca2+-dependent modulation of voltage-gated myocyte sodium channels. Biochem Soc Trans 2021 Nov 1;49(5):1941-1961. doi: 10.1042/BST20200604. PMID: 34643236; PMCID: PMC8589445.
29. Vimalraj SA. Concise review of VEGF, PDGF, FGF, Notch, angiopoietin, and HGF signalling in tumor angiogenesis with a focus on alternative approaches and future directions. Int J Biol Macromol. 2022;221;1428-1438.
30. Cao R, Eriksson A, Kubo H, et al. Comparative evaluation of FGF-2-, VEGF-A-, and VEGF-C-induced angiogenesis, lymphangiogenesis, vascular fenestrations, and permeability. Circ Res. 2004 Mar 19;94(5):664-70. doi: 10.1161/01.RES.0000118600.91698.BB. 2004 Jan 22. PMID: 14739162.
31. Fletcher-Hall S. Pacemaker-induced cardiomyopathy. JAAPA. 2023 Sep 1;36(9):1-4. doi: 10.1097/01.JAA.0000947080.85880.bb. PMID: 37668488.
32. George I, Geddis MS, Lill Z, et al. Myocardial function improved by electromagnetic field induction of stress protein hsp70. J Cell Physiol. 2008 Sep;216(3):816-23. doi: 10.1002/jcp.21461. PMID: 18446816; PMCID: PMC3075533.
33. Wang S, Chen J, Chen MT, et al. Cardiac myocyte excitation by ultrashort high-field pulses. Biophys J. 2009 Feb 18;96(4):1640-8. doi: 10.1016/j.bpj.2008.11.011. PMID: 19217879; PMCID: PMC2717245.
34. Guo HD, Wu JH, Wang HJ, et al. Delivery of Stem Cells and BMP-2 With Functionalized Self-Assembling Peptide Enhances Regeneration of Infarcted Myocardium. Stem Cell Rev Rep. 2024 Aug;20(6):1540-1554. doi: 10.1007/s12015-024-10721-7. Epub 2024 Apr 24. PMID: 38656478.
35. Andrée B, Duprez D, Vorbusch B, et al. BMP-2 induces ectopic expression of cardiac lineage markers and interferes with somite formation in chicken embryos. Mech Dev. 1998 Jan;70(1-2):119-31. doi: 10.1016/s0925-4773(97)00186-x. PMID: 9510029.
36. Wang S, Sun A, Li L, et al. Up-regulation of BMP-2 antagonizes TGF-β1/ROCK-enhanced cardiac fibrotic signalling through activation of Smurf1/Smad6 complex. J Cell Mol Med. 2012 Oct;16(10):2301-10. doi: 10.1111/j.1582-4934.2012.01538.x. PMID: 22283839; PMCID: PMC3823423.
37. Harakawa S, Hori T, Hiramoto T, et al. Suppression of Glucocorticoid Response in Stressed Mice Using 50 Hz Electric Field According to Immobilization Degree and Posture. Biology (Basel). 2022 Sep 9;11(9):1336. doi: 10.3390/biology11091336. PMID: 36138815; PMCID: PMC9495954.
38. Katoh K. Effects of Electrical Stimulation of the Cell: Wound Healing, Cell Proliferation, Apoptosis, and Signal Transduction. Med Sci (Basel). 2023 Jan 17;11(1):11. doi: 10.3390/medsci11010011. PMID: 36810478; PMCID: PMC9944882.
39. Song MY, Yu JZ, Zhao DM, et al. The time-dependent manner of sinusoidal electromagnetic fields on rat bone marrow mesenchymal stem cells proliferation, differentiation, and mineralization. Cell biochem and biophys. 2014;69;47-54.